IL NUOVO CIMENTO **38 C** (2015) 12
DOI 10.1393/ncc/i2015-15012-7

COLLOQUIA: IFAE 2014

Results and perspectives of the MEG and MEG II experiments

MARCO VENTURINI on behalf of the MEG COLLABORATION

Scuola Normale Superiore - Piazza dei Cavalieri 7, 56126 Pisa, Italy and
INFN, Sezione di Pisa - Largo B. Pontecorvo 3, 56127 Pisa, Italy

received 7 January 2015

Summary. — Charged-lepton-flavour–violating decays are prohibited in the framework of the Standard Model of elementary particles, but many of its extensions predict measurable values for such decays. Several experiments are running or being designed to measure (or to set a limit on) such processes. Among these, the MEG experiment has recently set a new upper limit on the $\mu \to e\gamma$ branching ratio $\mathcal{B} < 5.7 \times 10^{-13}$ at 90% CL. The process has a simple kinematics but very good resolutions are needed for discarding the huge background. In order to improve its sensitivity, an upgrade of the experiment is under development, and will start taking data in 2016. The foreseen sensitivity of the upgraded apparatus will be about 5×10^{-14} on the branching ratio of the process.

PACS 13.35.Bv – Decays of muons.
PACS 29.40.-n – Radiation detectors.

1. – Lepton flavour and new physics

In the Standard Model, the assumption of massless neutrinos leaves no room for lepton flavour changing processes. The experimental evidence of neutrino oscillations, as a manifestation of the non-zero masses of neutrinos, makes flavour transitions possible in the charged sector as well. However an unmeasurably small probability is predicted for such processes [1]: what really suppresses such amplitudes is the requirement for neutrinos to oscillate during a W's lifetime, yielding a suppression factor $\approx (m_\nu/m_W)^4$. Among the charged-lepton-flavour–violating processes, the $\mu \to e\gamma$ decay plays a key role in the search for new physics [2]. From a theoretical point of view, it has no Standard Model background, so the measurement of new physics contributions does not depend on theoretical predictions with uncertainties coming from hadron physics or high-order contributions. From an experimental point of view the use of muons presents some advantages: muons are easy to produce, have an almost-macroscopic mean life and a very limited number of decay channels.

The interest in searching for the $\mu \to e\gamma$ decay is also driven by many models beyond the Standard Model which predict branching ratios of about 10^{-12}–10^{-14}. Such values

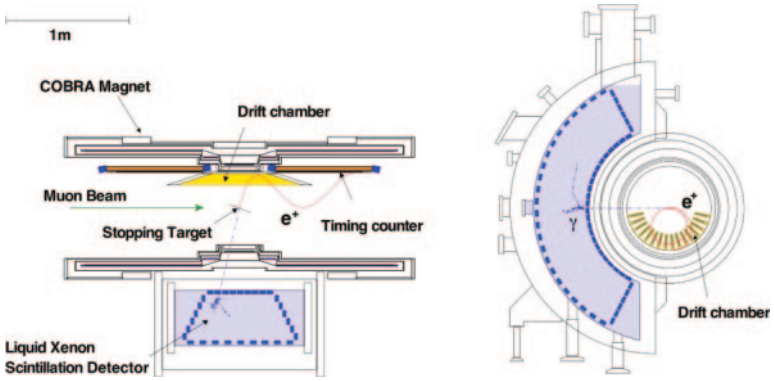

Fig. 1. – Schematic view of the MEG experiment with a signal event displayed.

are in the range of the sensitivities achieveable with present detector technology. In addition, the amplitude of the $\mu \to e\gamma$ process is related in several models to other key observables, such as the muon anomalous magnetic moment and the neutrino mixing angle ϑ_{13}, thus spanning large parts of the parameter spaces of the theories with parallel measurements.

2. – The MEG experiment

The MEG experiment searches for the $\mu \to e\gamma$ decay at the Paul Scherrer Institut (PSI) near Zurich, Switzerland. It represents the last step of a 60-year search started in the 1940s by Hincks and Pontecorvo with cosmic muons. Several dedicated experiments followed with the peculiarity of being small experiments ("table-top") with detectors at the leading-edge of technology.

2˙1. *Event signature and background*. – The $\mu \to e\gamma$ decay has a very simple kinematic signature: it is a two-body decay, so in the reference frame where the muon is at rest the electron and the photon have the same energy, equal to half of the muon mass $E = m_\mu/2 = 52.83\,\mathrm{MeV}$, and are emitted back-to-back.

Two sources of background can mimic the signal signature: a correlated background, coming from muon radiative decays $\mu \to e\nu\bar{\nu}\gamma$ when neutrinos carry a little energy; an accidental background, consisting in a detection of a positron coming from muon normal decays in coincidence with an uncorrelated photon with energy, angle and timing compatible with those of a signal event. The contribution of accidental background has a strong dependence on the muon stopping rate, and in MEG is actually the main source of background. Nevertheless the ultimate discrimination of signal over noise is dictated by detector resolutions on the kinematic quantities that identify a $\mu \to e\gamma$ event: photon and positron energy, their relative angle and timing.

2˙2. *The detector*. – The MEG apparatus, sketched in fig. 1, is tailored to take advantage of the well-defined kinematics of the $\mu \to e\gamma$ process [3]. The most intense continuous muon beam of the world is provided by PSI, which for MEG is tuned to $3 \times 10^7\,\mu^+/\mathrm{s}$ with an average momentum of $28\,\mathrm{MeV}/c$. The beam rate is limited in order to keep accidental background contribution under control. The beam is stopped in a $205\,\mu\mathrm{m}$ polyethylene target. The emerging positrons are tracked by a magnetic spectrometer composed of a

TABLE I. – *Measured resolutions for MEG and expected for MEG II. u is along the beam axis; v is directed along the inner face from bottom to top; w measures the depth from the inner face.*

Variable	MEG	MEG II
ΔE_γ(%)	1.7	1.0
γ position (mm)	5(u, v), 6(w)	2.6(u), 2.2(v), 5(w)
ΔP_e (keV)	306	130
e^+ angle (mrad)	7(φ_e), 9.4(ϑ_e)	5.3(φ_e), 3.7(ϑ_e)
$\Delta t_{e\gamma}$ (ps)	122	84
e^+ efficiency (%)	40	88
γ efficiency (%)	63	69
trigger efficiency (%)	99	99

set of drift chamber modules and a couple of timing counters, immersed in a non-uniform magnetic field provided by the COBRA superconducting magnet. Photons are measured by a liquid xenon detector, which is used to determine their energy, time and conversion point.

The non-uniformity of the COBRA magnetic field cancels the dependence of the positron bending radius on the emission angle (COnstant Bending RAdius) and strongly reduces the occupancy of the drift chambers by sweeping away particles with low longitudinal momentum. The drift chamber system is composed of 16 modules, placed in a half circle with radial orientation. The single module has a trapezoidal shape and contains two independent detector planes, made of an array of alternating field and sense wires enclosed by two cathode foils each, equipped with Vernier pads for charge division measurements. The modules are filled with a helium-ethane gas mixture 50:50, while the remaining volume inside COBRA is filled with pure helium. Two identical hodoscopes (timing counters) are placed at the two sides of the drift chambers along the beam axis for the determination of positron time. Each hodoscope consists of a layer of scintillating fibres, read out by avalanche photodiodes, placed on the top of an array of 15 scintillating bars, which are coupled to fine-mesh fast photomultipliers. Bars and fibres are oriented perpendicularly, with the bars being parallel to the beam axis.

The photon detector is a homogeneous calorimeter with 900 l of liquid xenon surrounded by 846 vacuum-ultra-violet sensitive photomultipliers, and placed in a cryostat that keeps xenon temperature stable at about 165 K. Liquid xenon has small radiation length ($X_0 = 2.7$ cm) and high light yield (the energy deposit needed for the emission of a scintillation photon is about 20 eV). These characteristics confer to xenon high detection efficiency, small leakage for electromagnetic showers and good energy resolution. In addition, all the three main mechanisms involved in scintillation have time constants below 50 ns. Such a fast response results in reduced pileup probability and in a superior timing resolution (of less than 100 ps). Its acceptance for photons emerging from the target is about 11%, and this sets the acceptance of the apparatus.

For the measurement and the monitor of the apparatus performance a rich set of calibrations has been developed. They involve both single detectors (energy scale, resolution variations...) and their intercalibration. They are performed with not only the muon beam but also with a positron beam, cosmic rays and gamma lines resulting from nuclear interactions induced by protons from a Cockcroft-Walton accelerator. The overall resolutions of the MEG detector on the kinematic variables are reported in table I.

In MEG the trigger is implemented in a cascaded custom made VME boards, performing a basic event reconstruction with signals from xenon detector and timing counters. Signals from the detectors are digitized by a waveform digitizer chip, the Domino Ring Sampler 4 (DRS4). This is necessary to exploit the detectors timing resolutions and to reduce the pile up of events.

2˙3. *The analysis*. – For the measurement of the branching ratio of the process a likelihood analysis is performed [4]. The distribution of events is studied in terms of 5-dimensional vectors $\vec{x} = (E_\gamma, E_e, t_{e\gamma}, \vartheta_{e\gamma}, \varphi_{e\gamma})$. The analysis follows a blinding procedure: events falling in a precise blinding window containing the signal region are written in separate files which are not opened until the analysis procedure is completely defined. The first step of the analysis is the determination of the Probability Density Functions (PDFs) for signal $S(\vec{x})$, radiative backgrounds $R(\vec{x})$ and accidental background $B(\vec{x})$, using both calibration data and background distributions in the sidebands. Once the PDFs are determined, the number of signal, radiative decay and accidental events (N_{sig}, N_{RMD}, N_{ACC}) are extracted by maximizing the following likelihood function:

$$\mathcal{L}(N_{\mathrm{sig}}, N_{\mathrm{RMD}}, N_{\mathrm{ACC}}) = \frac{e^{-N}}{N_{\mathrm{obs}}!} \prod_{i=1}^{N_{\mathrm{obs}}} \left[N_{\mathrm{sig}}\, S(\vec{x}_i) + N_{\mathrm{RMD}}\, R(\vec{x}_i) + N_{\mathrm{ACC}}\, B(\vec{x}_i)\right] \times \exp\left[-\frac{(N_{\mathrm{RMD}} - \langle N_{\mathrm{RMD}}\rangle)^2}{2\sigma^2_{\mathrm{RMD}}}\right] \exp\left[-\frac{(N_{\mathrm{ACC}} - \langle N_{\mathrm{ACC}}\rangle)^2}{2\sigma^2_{\mathrm{ACC}}}\right],$$

where N_{obs} is the number of events detected in the signal window and $N = N_{\mathrm{sig}} + N_{\mathrm{RMD}} + N_{\mathrm{ACC}}$.

From sideband studies we get an estimate of the number of background events in the signal region $\langle N_{\mathrm{RMD,ACC}}\rangle$ with a corresponding variance $\sigma^2_{\mathrm{RMD,ACC}}$. This additional measurement is included in the analysis by means of the two Gaussian terms in the likelihood function. For the determination of the branching ratio, the number of measured events is normalized to the number of Michel positrons passing the same selection criteria. The computation of the confidence interval is based on Feldman-Cousins approach with a profile likelihood-ratio ordering.

With the analysis of data collected in the period 2009–2011, an upper limit on the branching ratio of 5.7×10^{-13} was obtained at 90% of confidence level. The analysis of remaining half of the collected statistics (corresponding to 2012–2013) is in progress, and the result will be published within 2015. With the full data set, MEG has reached the ultimate sensitivity dictated by the background. A substantial improvement of MEG results requires an improvement of detector performances, in order to reject the background contributions which limit the signal sensitivity. This will be carried out by a short-term upgrade of the apparatus, MEG II [5].

3. – The MEG II experiment

The major modifications of MEG apparatus are shown in fig. 2: the drift chamber and the timing counters are completely replaced while the calorimeter undergoes substitutions and rearrangements of the photosensors.

The new positron spectrometer consists of a hyperbolic drift chamber and two pixelated timing counters. In the new configuration positrons traverse less material along their path, and the capabilities of matching the information from the two detectors are

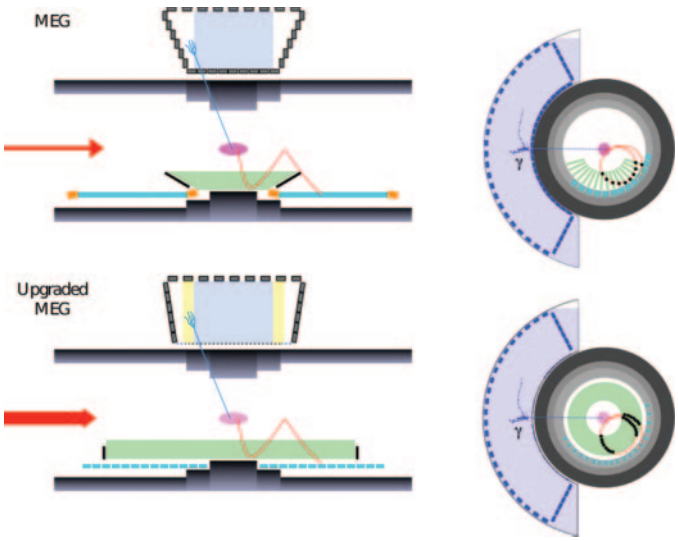

Fig. 2. – Improvements of the MEG detector.

powered. The hyperbolic profile of the chamber along the beam axis comes from the stereo configuration of wires, which form a stereo angle varying from 8° in the outermost layers to 7° in the innermost ones. The 10 sense wire planes, each embedded between two field wire planes, have alternating stereo angles. Such configuration conveys information for reconstructing the longitudinal coordinate. The single drift cell has an approximately squared shape with a width of 7 mm, and has a sense wire placed at the centre surrounded by eight field wires. As counting gas a lowmass mixture of helium and isobutane will be used in the fractions 85:15. This allows the minimization of the total number of radiation lengths for the new tracker: 1.24×10^3 radiation lengths per track turn, to be compared with 1.7×10^3 for the MEG tracker.

The present timing counters cannot stand a positron rate increased by a factor 2–3. It is necessary to segment the detector: the proposed detector is a pixelated timing counter consisting of many scintillator tiles coupled to Silicon PhotoMultipliers (SiPMs). Light is collected by two SiPMs connected in series, whose signal is directly sent to a WaveDream board (the evolution for MEG II of the DRS4), a 2 GHz waveform digitizer. The segmentation of the timing counter brings an intrinsic potential in improving the timing resolution, coming from the possibility of averaging the positron hit time over the multiple hit pixels.

The main issue of MEG xenon calorimeter is the dependence of resolutions on the depth of the γ-conversion. This is due to the granularity of the $2''$ PMTs on the front face distributed in a mesh of 6.2 cm side, therefore in MEG II the PMTs in the entrance face will be replaced by smaller photosensors, $1 \times 1\,\mathrm{cm}^2$ SiPMs. The imaging power is thus greatly increased. The layout of the lateral faces will be modified too in order to avoid shadow areas, which result in a reduced acceptance. The proposed structure is visible in fig. 2, where the wider acceptance region is highlighted.

In table I we report resolutions measured in MEG and expected for MEG II. Better detector resolutions will permit a higher beam rate, about $7 \times 10^7\,\mu$/s. In three years of data taking MEG II expected sensitivity is about 5×10^{-14} on the branching ratio of $\mu \to e\gamma$. The detector will be ready for an engineering run within 2015.

4. – Conclusions

Charged Lepton Flavour Violation (CLFV) experiments represent a powerful tool to investigate new physics scenarios with no SM background. Combined measurements on CLFV processes can significantly constrain new physics at high energy scales. The MEG experiment has recently set the most stringent limit on CLFV physics scenarios and in a few years MEG II will improve MEG results by an order of magnitude.

REFERENCES

[1] Bilenky S. M., Petcov S. T. and Pontecorvo B., *Phys. Lett. B*, **67** (1977) 309.
[2] Kuno Y. and Okada Y., *Rev. Mod. Phys.*, **73** (2001) 151.
[3] Adam J. *et al.*, *Eur. Phys. J. C*, **73** (2013) 2365.
[4] Adam J. *et al.*, *Phys. Rev. Lett.*, **110** (2013) 201801.
[5] Baldini A. M. *et al.*, arXiv:1301.7225.